Dopant Structure in $FeCl_3$-doped Polyacetylene Studied by X-Ray Absorption Spectroscopy and X-Ray Photoelectron Spectroscopy

Kiyotaka Asakura, Isao Ikemoto,† Haruo Kuroda,* Takaaki Kobayashi,†† and Hideki Shirakawa††
Department of Chemistry and Research Center for Spectrochemistry, Faculty of Science, The University of Tokyo, Hongo, Bunkyo-ku, Tokyo 113
††*Institute of Material Science, University of Tsukuba, Sakura-machi Niihari-gun, Ibaragi 305*

(Received March 18, 1985)

The dopant structure in $FeCl_3$-doped polyacetylene was studied from the analysis of Fe K-edge EXAFS and XANES, measured by use of synchroton radiation. It is concluded that Fe atom is surrounded by four Cl atoms with Fe–Cl distance of 2.19—2.20 Å, and the dopant exists in the state of $[FeCl_4]^-$. The following mechanism is proposed for the doping process:

$$(CH)_x + 2yxFeCl_3 \rightarrow [CH(FeCl_4^-)_y]_x + yxFeCl_2$$

It is also shown that the chlorination of polyacetylene occurs significantly on performing a "heavy doping."

When doped with a suitable electron donor or acceptor, polyacetylene becomes metallic with an electrical conductivity more than 12 orders of magnitude higher than that of the undoped state.[1] A wide variety of dopants has been tested to see their effects on the electrical properties. However, little has been known on the electronic states and geometrical structures of dopants in the doped polyacetylenes. When a polyacetylene film is immersed into a nitromethane solution of $FeCl_3$, $FeCl_3$ is taken into the polyacetylene film to give electrical conductivity of, at most, $10^2\ S\ cm^{-1}$.[2,3] The state of the dopant in the $FeCl_3$-doped polyacetylene was studied by means of Mössbauer spectroscopy and ESR, but there were some contradictions among the conclusions given by different authors.[4–7]

The doping of polyacetylene is often compared with the formation of the graphite intercalation compound. In the case of the graphite intercalation compound with $FeCl_3$, the intercalated $FeCl_3$ layer was reported to have a structure more or less similar to that in anhydrous $FeCl_3$.[8] On the other hand, available experimental data suggest that the dopant state in $FeCl_3$-doped polyacetylene is quite different from this case.[4–7] Thus it seemed to be of great interest to elucidate the dopant structure in a $FeCl_3$-doped polyacetylene. We report here the results of the analysis of the extended X-ray absorption fine structure (EXAFS) and X-ray absorption near-edge structure (XANES) of Fe K-edge measured on $FeCl_3$-doped polyacetylene films. They provide a most direct evidence that the dopant exists in the state of $[FeCl_4]^-$. Curious behaviors were found for a heavy doping with $FeCl_3$. Namely, Fe K-edge jump decreased in spite of the increase of apparent dopant content, and the electrical conductivity of the film decreased on increasing apparent dopant content. We will also discuss the origin of this phenomenon.

Experimental

Polyacetylene films of cis-rich form were prepared by the previously reported method.[9] $FeCl_3$-doping was carried out by immersing polyacetylene films into a nitromethane solution of $FeCl_3$ as described elsewhere.[3] $FeCl_3$ had been kept *in vacuo* for several hours before use. Nitromethane was well dried over $CaCl_2$ and distilled before it was used as the solvent. Films of different dopant content were obtained by changing the immersing period and/or $FeCl_3$ concentration of the solution. The dopant contents and electrical conductivities of the prepared samples are listed in Table 1. The dopant content given there is the apparent value which is calculated from the weight uptake of a polyacetylene film in the doping process assuming that the dopant exists entirely in the form of $FeCl_3$. In reality, the dopant exists as $[FeCl_4]^-$, not as $FeCl_3$, and furthermore, the weight increase is partly due to the chlorination of polyacetylene, particularly in the case of heavy doping as we will show later. Thus the values of dopant content in Table 1 should be taken only as a measure of doping degree. Figure 1 shows the change of electrical conductivity as a function of dopant content, where the points indicated as **A**, **B**, **C**, and **D** correspond to Samples **A**, **B**, **C**, and **D**, respectively.

The specimens for the measurements of X-ray absorption spectrum were prepared in the following way. In an Ar-

Table 1. The dopant content and conductivity of $FeCl_3$-doped polyacetylene sample

Sample	Dopant concent[a)] % mol/(CH) mol	Conductivity S/cm
Sample **A**	2.4	10—80
Sample **B**	8.7	700—800
Sample **C**	13.0	0.4—200
Sample **D**	7.4	700

a) Dopant content was calculated from the weight uptake of the polyacetylene assuming all the dopant was in the form of $FeCl_3$.

---

† Present address: Department of Chemistry, Faculty of Science, Tokyo Metroporitan University, Fukasawa, Setagaya-ku, Tokyo 158.

filled gloved box, a doped polyacetylene film was cut into several pieces of appropriate size and folded up several times to give a thickness suitable for X-ray absorption measurement, and then sandwiched between two pieces of adhesive tape to keep it in the folded state and, at the same time, to prevent the sample from a direct exposure to the atmosphere. The samples prepared by this way were stored in an Ar-filled Schlenk flask until just before they were used for the measurements.

Preliminary EXAFS experiments were done by use of an in-laboratory EXAFS spectrometer combined with a high-power rotating-anode X-ray generator (RIGAKU RU-1000).[10] Through these experiments, we checked the effects of sealing the sample with adhesive tapes, the appropriate sample thickness, and the homogeneity of the dopant distribution in a doped film. The final data of X-ray absorption spectrum were taken by use of synchrotron radiation emitted from the 2.5 GeV storage ring of the Photon Factory in the National Laboratory for High-energy Physics (KEK-PF), employing the EXAFS facilities at BL-10B.[11] X-Rays were monochromatized with a Si(311) channel-cut crystal. The intensity of the incident beam, I_0, and that of the transmitted beam, I, were measured with the ionization chambers which were placed before and after the sample, respectively, the gas filled in an ionization chamber being N_2 for I_0 and Ar for I. Most of X-ray absorption measurements were done at room temperature. The measurement at low temperature (10 and 80 K) was done only for Sample **D**, which was regarded to be a representative sample having a high electrical conductivity. X-Ray photoelectron spectra were taken with McPherson ESCA 36 electron spectrometer by empolying Mg*Kα* (1253.6 eV) as the stimulating radiation. In order to avoid the effects of directly exposing the sample to air, a sample which has been kept in an Ar-filled vessel was transferred to the spectrometer by use of an Ar-filled gloved box which was directly connected to the spectrometer. The gases coming out from a sample were analyzed by use of JEOL JMS-D300 mass spectrometer. For the purpose to check the inhomogeneity of Fe distribution in a $FeCl_3$-doped polyacetylene film, we carried out the electron probe microanalysis by use of JEOL EPXMA TYPE JXA-5, the intensity distribution of Fe*Kα* fluorescent X-ray being observed.

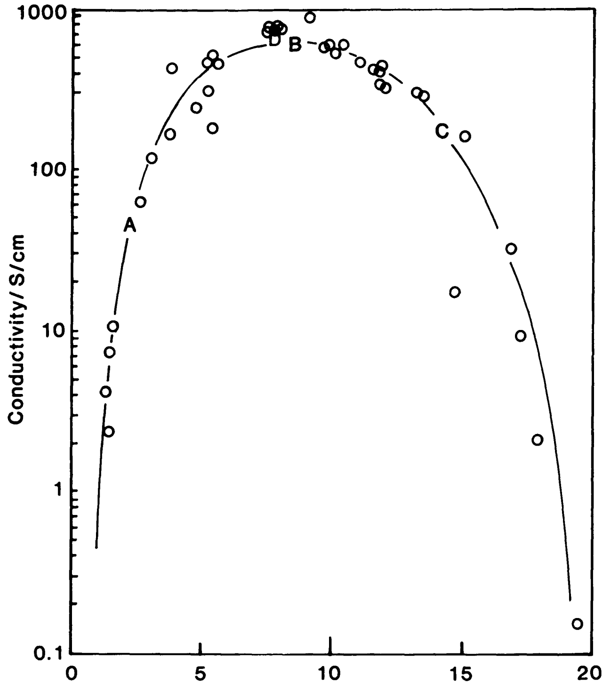

Fig. 1. Conductivity of $FeCl_3$-doped polyacetylene as a function of dopant concentration y. **A**, **B**, and **C** in the figure correspond to samples **A**, **B**, and **C**, respectively.

Results and Discussion

In the preliminary EXAFS experiments, we noted that Fe K-edge jump was significantly lower in the case of Sample **C** than what was expected from its apparent dopant content, it being even lower than those observed for Samples **A**, **B**, and **D**, and furthermore, it was found to vary as we examined different portions of Sample **C**. Since the latter fact indicated that the distribution of Fe is considerably inhomogeneous in this sample, we examined the Fe distribution in the film by use of an electron probe microanalyzer (EPMA). The image of Fe*Kα* fluorescent X-ray showed that Fe distribution was indeed quite inhomogeneous, having Fe-rich regions and Fe-less regions within a film. On the other hand, the films of lower dopant content (Samples **A**, **B**, and **D**) were found to have a homogeneous Fe distribution. The reason for this anomarous behavior of Sample **C** will be discussed later.

As a typical example of the Fe K-edge absorption spectra measured by use of synchrotron radiation, the spectrum of Sample **D** at 80 K is shown in Fig. 2. The spectrum shows a sharp pre-edge peak attributable to ls-3d transition and several peaks near Fe K-edge,

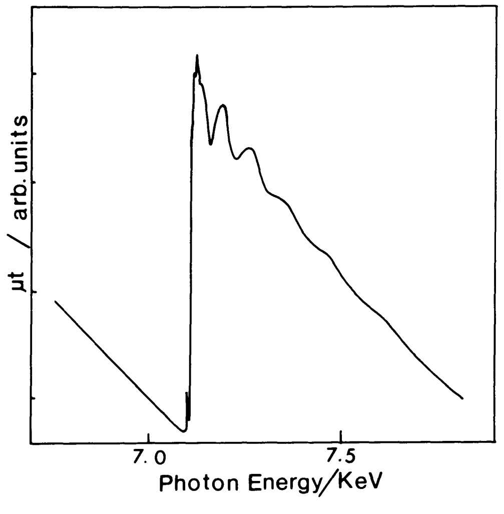

Fig. 2. Fe K absorption spectrum of Sample **D** at 80 K.

which are followed by EXAFS of a relatively simple structure. Spectral shape was found to be almost the same for all other samples of $FeCl_3$-doped polyacetylene.

We extracted EXAFS oscillation $\chi(k)$ from the observed spectra by the following method.[12] The smoothly-varying component $\mu_s(\lambda)$, was estimated by fitting an observed spectrum using the cubic spline method. The free atom absorption coefficient, $\mu_0(\lambda)$, in the region of 50—60 eV from the edge was taken to be equal to the difference between μ_s and the background absorption μ_b which was determined by a smooth extrapolation from the preedge region by use of Eq. 1.

$$\mu_b(\lambda) = \mathbf{A} + \mathbf{C}\lambda^3 + \mathbf{D}\lambda^4 \quad (1)$$

The μ_0 value in other region was estimated by extrapolating the μ_0 values in the above-mentioned region assuming that the wavelength dependence of μ_0 was describable with the Victoreen's equation, the parameters of which were taken from the literature.[13] The photon energy E was converted to the photoelectron wave number k by Eq. 2.

$$k = \sqrt{2m(E-E_0)}/\hbar \quad (2)$$

where E_0 is the ionization threshold. Then the EXAFS oscillation was calculated by using Eq. 3.

$$\chi(k) = (\mu-\mu_s)/\mu_0 \quad (3)$$

Using thus extracted $\chi(k)$, we performed a Fourier transformation of $k^3\cdot\chi(k)$ over the region, $4 \leqq k \leqq 12$ Å^{-1}.

Figure 3 shows the Fourier transform of the EXAFS data of Sample **D** at 80 K. It shows only one prominent peak with the maximum at about 1.8 Å. This peak can be attributed to the nearest-neighbor Cl atoms surrounding Fe atom. No peak which is attributable to Fe–C or Fe–Fe, can be found even in the Fourier transform of the EXAFS data at 10 K. The Fourier transforms of the EXAFS data of all other samples (Samples **A**, **B**, and **C**) were also nearly the same as that of Sample **D**, exhibiting again only one prominent peak attributable to Fe–Cl.

Assuming the first shell to be due to Fe–Cl bond, we carried out the curve-fitting analysis by use of the following equation based on the single scattering theory.

$$k^3\chi(k) = (N/R^2)k^2F(k)\exp(-2k^2\sigma^2)\sin[2kR+\phi(k)] \quad (4)$$

where N is the coordination number, R the interatomic distance, $F(k)$ the back-scattering amplitude function, σ the Debye-Waller factor, $\phi(k)$ the phase shift function. The back-scattering amplitude function $F(k)$ and the phase shift function $\phi(k)$ were empirically determined from the analysis of the EXAFS data of the model compound, $[N(C_2H_5)_4][FeCl_4]$. Treating N, R, and σ as fitting parameters, their best-fit values were determined by means of the nonlinear least square technique. Figure 4 shows the calculated and observed $k^3\cdot\chi(k)$ curves for Sample **D**. The R and N values obtained by the curve-fitting analysis are listed in Table 2. For all samples of $FeCl_3$-doped polyacetylene, Fe–Cl bond length was found to be 2.19—2.20 Å. The obtained coordination numbers were somewhat different from sample to sample within the range of 3—4. But this difference is not likely to be intrinsic since a relatively large error is generally expected for a coordination number determined from the EXAFS data measured at room temperature. Because the EXAFS data obtained at lower temperature have better quality, the coordination number 3.9—4.0 obtained from the 80 K and 10 K EXAFS data of Sample **D**, is most reliable and can be taken as the actual coordination number. Thus we can conclude that, in the $FeCl_3$-doped

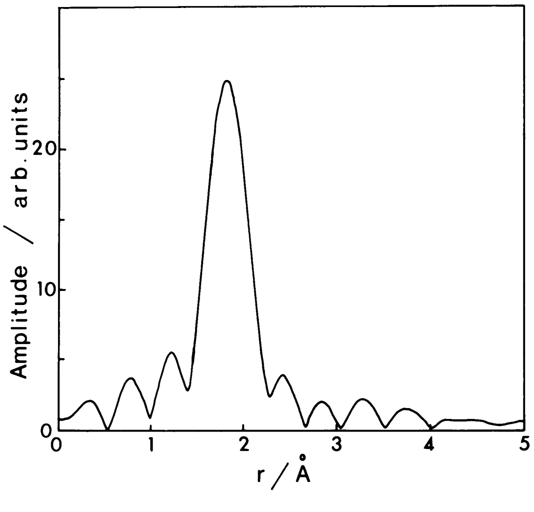

Fig. 3. Fourier transform of $k^3\cdot\chi(k)$ of the 80 K EXAFS data of Sample **D**.

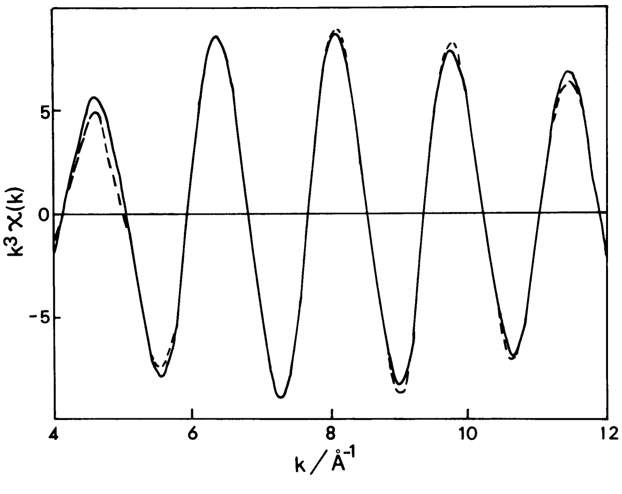

Fig. 4. The calculated (——) and observed (- - -) $k^3\cdot\chi(k)$ curves for Sample **D**.

polyacetylene, Fe atom is surrounded by four Cl atoms with Fe–Cl distance of 2.19—2.20 Å.

There are several kinds of the chemically stable ion of the type $[FeCl_x]^{y-}$, which are $[FeCl_4]^-$, $[FeCl_4]^{2-}$, $[FeCl_6]^{3-}$, and $[FeCl_6]^{4-}$. The Fe–Cl distances which have been determined from the crystal structure analysis are given in Table 3. Note that Fe–Cl distance is nearly the same for a given kind of the anion irrespective of the kind of the counter cation. In other words, it is almost determined by the valence state of Fe and the Cl coornination number. The data shown in Table 3, indicate that the Fe–Cl distance of 2.19 Å is the one characteristic of $[FeCl_4]^-$. Another ion which has the coordination number of 4, is $[FeCl_4]^{2-}$, but its average Fe–Cl distance is about 2.3 A. Therefore the results of the analysis of the Fe K-edge EXAFS data of $FeCl_3$-doped polyacetylenes indicate that the dopant is in the state of $[FeCl_4]^-$. As we have mentioned, Sample **C** has a very inhomogeneous Fe distribution. However, its Fe K-edge EXAFS data gave also the same conclusion. This means that the Fe-containing chemical species existing in the Fe-rich regions of this sample is also in the state of $[FeCl_4]^-$.

As it is known, XANES is determined by the local electronic state surrounding the X-ray absorbing atom, and reflects the valency state and the local symmetry around the X-ray absorbing atom.[23,24] Although a detailed analysis of XANES is rather complicated, one can use XANES just as a fingerprint of the local structure and electronic state. In Fig. 5, the Fe K-edge XANES spectrum of Sample **D** measured at 80 K is compared with the corresponding spectra of $[Co(NH_3)_6][FeCl_6]$, $[N(C_2H_5)_4]_2[FeCl_4]$, and $[N(C_2H_5)_4][FeCl_4]$, in which the local structure surrounding Fe is $[FeCl_6]^{3-}$, $[FeCl_4]^{2-}$, and $[FeCl_4]^-$, respectively. The sharp pre-edge peak in the spectrum of Sample **D** arises from 1a—3d transition and is characteristic of a tetrahedrally-coordinated ion like $[FeCl_4]^-$. Furthermore, the structures above the absorption edge are also similar to the ones found for $[N(C_2H_5)_4][FeCl_4]$. XANES spectra of other $FeCl_3$-doped samples are also nearly the same as that of Sample **D**. Thus the Fe K-edge XANES of $FeCl_3$-doped polyacetylene indicates that the local state surrounding Fe corresponds to $[FeCl_4]^-$ in agreement with the conclusion derived from EXAFS data. Summarizing all the results mentioned above, we can definitely conclude that, in a $FeCl_3$-doped polyacetylene, the dopant exists mainly in the state of $[FeCl_4]^-$,

Table 2. Results of the analysis of EXAFS data by using the empirical parameters[a)]

Sample		Bond length l/Å	Coordination No.
Sample **A**		2.200	2.9
Sample **B**		2.195	3.3
Sample **C**		2.195	4.2
Sample **D**	(T=300 K)	2.199	3.5
Sample **D**	(T= 80 K)	2.200	3.9
Sample **D**	(T= 10 K)	2.200	4.0

a) The phase shift and amplitude functions obtained from the analysis of the room-temperature EXAFS data of $[N(C_2H_5)_4][FeCl_4]$, assuming Fe–Cl distance as 2.18 Å and coordination number as 4, were used except for the analyses of the 80 K and 10 K EXAFS data of Sample **D**, for which the empirical parameters derived from the 80 K EXAFS data of $[N(C_2H_5)_4][FeCl_4]$.

Table 3. Fe–Cl bond lengths in $[FeCl_x]^{y-}$ ions

Type	Salt	Bond length l/Å	Ref
$[FeCl_4]^{2-}$	$(C_5H_5S_2)_2[FeCl_4]$	2.313 (av.)	14
	$(C_5H_5S_2)_2[FeCl_4]$	2.33 (av.)	15
	$\{[Fe(\eta^5\text{-}C_5H_5)(CO)_2]_3SbCl\}_2$ $[FeCl_4]CH_2Cl_2$	2.302 (av.)	16
	$[N(CH_3)_4]_2[FeCl_4]$	2.292	17
$[FeCl_4]^-$	$[As(C_6H_5)_4[FeCl_4]$	2.19	18
	$[FeCl_2(DMSO)_4][FeCl_4]$	2.162	19
	$Na[FeCl_4]$	2.196	20
	$[PCl_4][FeCl_4]$	2.185	21
$[FeCl_6]^{4-}$	$NaK_3[FeCl_6]$	2.5100	22
$[FeCl_6]^{3-}$	$[Co(NH_3)_6][FeCl_6]$	2.3926	22

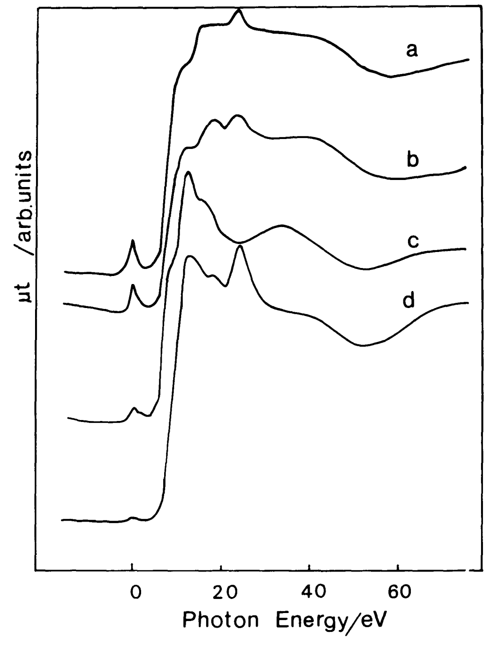

Fig. 5. XANES spectra of (a) Sample **D**, (b) $[N(C_2H_5)_4][FeCl_4]$, (c) $[N(C_2H_5)_4]_2$ $[FeCl_4]$ and (d) $[Co(NH_3)_6][FeCl_6]$. The photon energy is measured from the transition energy of the pre-edge peak E_a of each sample. The transition energies of the pre-edge peaks of Sample **D**, $[N(C_2H_5)_4][FeCl_4]$, $[N(C_2H_5)_4]_2$ $[FeCl_4]$ and $[Co(NH_3)_6]$ $[FeCl_6]$ are 7104.8, 7104.8, 7103.0, and 7104.5 eV, respectively.

not in the state of $FeCl_3$ nor in the state of $[FeCl_4]^{2-}$. This conclusion is consistent with the recent studies by Mössbauer spectroscopy.[4,5]

The dopant state revealed by the present study, is quite different from that in the graphite intercalation compound, where ther intercalated $FeCl_3$ takes a layer structure somewhat similar to the one in anhydrous $FeCl_3$, having a partial charge transfer between graphite and $FeCl_3$ layers.[8] Since the dopant exists as $[FeCl_4]^-$, we propose the following doping mechanism for the $FeCl_3$-doped polyacetylene. In a separate experiment, we have studied the solute structure in a nitromethane solution of $FeCl_3$ by use of Fe K-edge EXAFS, and found that $[FeCl_4]^-$ exists in the nitromethane solution beside another iron-containing species.[25] The latter is likely to be a solvated octahedral chloro complex,[25] which we tentatively denote as $[FeCl_2]^+$. Possibly the following electrolytic dissociation had taken place in the nitromethane solution to yield $[FeCl_4]^-$.

$$2FeCl_3 \rightarrow [FeCl_4]^- + [FeCl_2]^+ \qquad (5)$$

Therefore it is most likely that, when a polyacetylene film is immersed into the nitromethane solution of $FeCl_3$, $[FeCl_2]^+$ is reduced by the electron transfer from polyacetylene to form $FeCl_2$ which might remain in the solution or precipitate from the solution, and only $[FeCl_4]^-$ ions enter into the space surrounded by positively-charged polyacetylene chains.

As shown in Fig. 1, it has been generally observed that the electrical conductivity of $FeCl_3$-doped polyacetylene initially increases with dopant content, but decreases when the apparent dopant content exceeds about 10 mol% on performing a heavy doping. Among the samples taken up in the present study, Sample **C** was the one prepared under the condition of heavy doping. In fact, the apparent dopant content of this sample was 13 mol%, which is considerably higher than that of Sample **D**. However, the magnitude of Fe K-edge jump was found to be lower in comparison with Sample **D**. As we have already mentioned, the magnitude of Fe K-edge jump varies from portion to portion on the film of Sample **C**. We confirmed also by means of electron probe microanalysis(EPMA), that Fe distribution is quite inhomogeneous in this sample. To clarify the origin of these anomalous behaviors of a heavily-doped sample, we examined the X-ray photoelectron spectra of $FeCl_3$-doped polyacetylene films. As shown in Fig. 6, Samples **A** and **B** exhibit a single C 1s peak accompanied by a high-binding-energy tail, whereas the C 1s spectrum of Sample **C** splits into two peaks, indicating the presence of two different kinds of C atom. The Cl 2p spectra of $FeCl_3$-doped polyacetylenes are shown in Fig.7 together with the corresponding spectrum of $[N(C_2H_5)_4][FeCl_4]$. Note that the Cl 2p spectrum of Sample **A** very much resembles that of $[N(C_2H_5)_4][FeCl_4]$, but the Cl 2p spectrum of Sample **C** exhibits a quite strange shape, indicating the presence of two different kinds of Cl atoms. The observed binding energies of C 1s and Cl 2p peaks are listed in Table 4. The binding energy of the main C 1s peak is 284.1 eV both for Sample **A** and Sample **B**, which is in good agreement with the C 1s binding energy of an undoped *trans*-polyacetylene. Since the C 1s spectrum of Sample **C** is clearly composed of two components, we carried out a deconvolution into two components and determined the energy splitting and the intensity ratio of the high-binding-energy com-

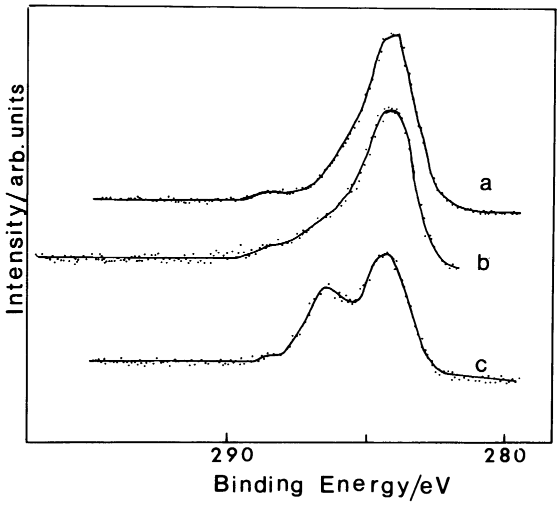

Fig. 6. XPS C_{1s} spectra of (a) Sample **A**, (b) Sample **B**, and (c) Sample **C**.

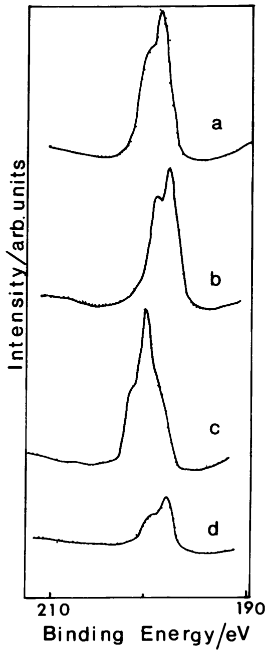

Fig. 7. XPS Cl_{2p} spectra of (a) Sample **A**, (b) Sample **B**, (c) Sample **C**, and (d) $[N(C_2H_5)_4][FeCl_4]$.

TABLE 4. XPS RESULTS OF $FeCl_3$-doped POLYACETYLENE FILMS

Sample	C_{1s}			Cl_{2p}		
	Binding energy		Intensity ratio	Binding energy		Intensity ratio
	C-1	C-2	C-2/C-1	Cl-1	Cl-2	Cl-2/Cl-1
	eV			eV		
Sample **A**	284.1	—	—	198.3	—	—
Sample **B**	284.1	—	—	198.2	—	—
Sample **C**	284.4	286.2	0.39	198.6	200.2	0.35

ponent to the low-binding-energy component. A deconvolution into two components was also done on the Cl 2p spectrum. The results are given in Table 4. Hereafter we denote the low-binding-energy component of the C 1s peak as C-1 and the high-binding-energy component as C-2. In the same way, we denote the low-binding-energy and high-binding-energy components of the Cl 2p spectrum as Cl-1 and Cl-2, respectively.

We noted that the shape of C 1s spectrum as well as that of Cl 2p spectum changed when Sample **C** was kept *in vacuo* for a long period (see Figs. 8 and 9). This means that the intensity ratio of the two components of each spectrum changes with time. In Fig. 10, we have plotted the intensity of each component as a function of the time for which the sample had been kept *in vacuo*. Note that the intensity of the C-2 component of the C 1s specrum decreased while that of the C-1 component increased with time, and at the same time, the intensity of the Cl-2 component of the Cl 2p spectrum showed a significant decrease with time while no appreciable

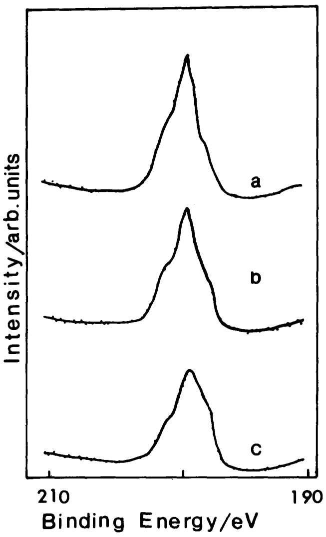

Fig. 9. Time dependence of the Cl_{2p} spectra of Sample **C**; (a) 11 h, (b) 25 h, (c) 50 h.

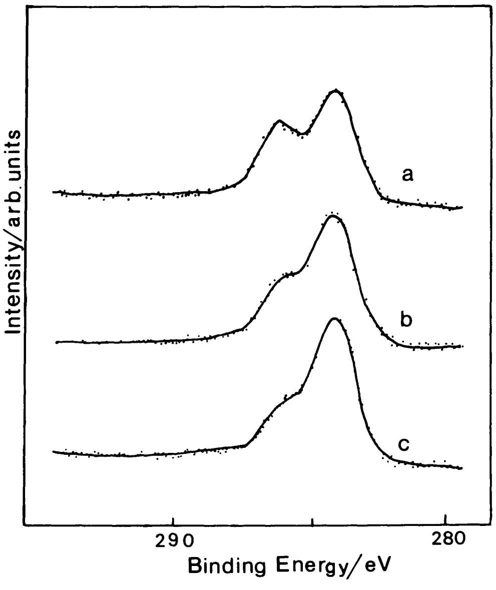

Fig. 8. Time dependence of the C_{1s} spectra of Sample **C**; (a) 10 h, (b) 24 h, and (c) 49 h.

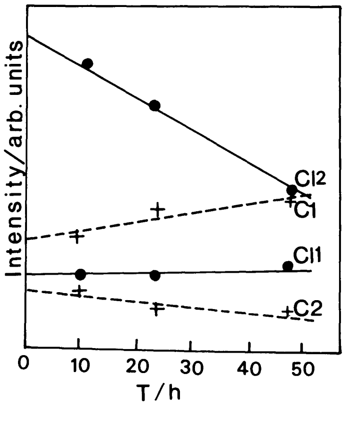

Fig. 10. Time dependence of the intensities of the decomvoluted components of Cl_{2p} and C_{1s} peaks. C-1 and C-2 denote the lower and higher binding energy components of the C_{1s} peaks, respectively. C-1 and Cl-2 denote the lower and higher binding energy components of Cl_{2p} peaks, respectively.

change was found for the intensity of the Cl-1 component. We examined the gases which coming from the sample during the above-mentioned process by use of mass spectroscopy and found that the main chemical species was HCl.

Summarizing the above-mentioned experimental data, we can derive the following conclusion. Since the intensities of the C-2 and Cl-2 components decrease in parallel to each other, they are likely to be associated with the same origin. The Cl $2p_{3/2}$ binding energy of the Cl-2 component, 200 eV, is the value that is usually found for a Cl atom forming C–Cl bond, and the C 1s binding energy of the C-2 component is the one that is expected for a C atom of C–Cl bond.[28] Thus the C-2 and Cl-2 components are likely to be associated with the C–Cl bond which has been formed as a result of the chlorination of polyacetylene chain. At present, we do not know about the mechamism of the chlorination taking place in the process of a heavy $FeCl_3$ doping. Possibly, when a polyacetylene film already saturated with $[FeCl_4]^-$ with apparent dopant content above 10 mol%, is further kept in a nitromethane solution of a high $FeCl_3$ concentration, the chlorination of polyacetylene chain takes place in some way within the doped region and the Fe containing species of the reaction products escapes from the polyacetylene film into the solution. Thus the weight increase in this process is not due to an increase of $[FeCl_4]^-$ content, but is mainly due to chlorination. This explains the reason why the magnitude of Fe K-edge jump is markedly smaller than what is expected from the apparent dopant content, and why the electrical conductivity decreases on a heavy doping.

The above-described phenomenon is similar in some respects to the one found for a heavy doping with bromine.[29] In this case, the addition of bromine to polyacetylene chain significantly takes place, resulting in an abrupt decrease of electrical conductivity. It is also known that HBr comes out from such a heavily Br-doped film when kept *in vacuo*.

Finally we wish to point out that, in the case of Sample **B** whose dopant content is just around 10 mol%, the shape of the Cl 2p spectrum is a little different from what is expected for $[FeCl_4]^-$. There seems to be a contribution of the component corresponding to Cl-2. In other words, the chlorination is likely to take place to a small extent even in a relatively-light $FeCl_3$ doping.

The authors would like to express their thanks for the technical advice given by Professor T. Matsushita, Dr. H. Oyanagi and Dr. M. Nomura on the measurements of EXAFS spectra at the Photon Factory. The analyses of EXAFS data were done by use of HITAC M-280H at the Computor Center, The University of Tokyo. This work was supported by the Grant-in-Aid for the Special Project Research on "the Properties of Molecular Assemblies" (No. 58118002), from the Ministry of Education, Science and Culture.

References

1) H. Shirakawa, E. J. Louis, A. G. MacDiarmid, C. K. Chiang, and A. J. Heeger, *J. Chem. Soc., Chem. Commun.*, **1977**, 578.

2) A. Pron, I. Kulszewicz, D. Billaud, and J. Przyluski, *J. Chem. Soc., Chem. Commun.*, **1981**, 783.

3) H. Shirakawa and T. Kobayashi, "Proceeding of International Conference on Physics and Chemistry of Conducting Polymer," Les arcs, France, (1982).

4) H. Sakai, Y. Maeda, T. Kobayashi, and H. Shirakawa, *Bull. Chem. Soc. Jpn.*, **56**, 1616 (1983).

5) Z. Kuoharski, M. Lukasiak, J. Suwalski, and A. Pron, to be published.

6) Y. W. Park, J. C. Woo, W. K. Han, C. H. Choi, T. Kobayashi, and H. Shirakawa, *Solid State Commun.*, **46**, 731 (1983).

7) A. Pron, P. Bernier, D. Billaud, and S. Lefrant, *Solid State Commun.*, **46**, 587 (1983).

8) a) W. Rudorff and H. Schulz, *Z. Anorg. Chem.*, **245**, 121 (1940); b) J. M. Cowley and J. A. Ibers, *Acta Cryst.*, **9**, 421 (1956).

9) T. Ito, H. Shirakawa, and S. Ikeda, *J. Polym. Sci., Polym. Ed.*, **13**, 1943 (1975).

10) Y. Sato, Thesis, The University of Tokyo (1982).

11) H. Oyanagi, T. Matsushita, M. Ito, and H. Kuroda, *KEK Report* **83—30**, (1984).

12) K. Asakura, M. Nomura, and H. Kuroda, *Bull. Chem. Soc. Jpn.*, **58**, 1543 (1985).

13) "International Tables for X-ray Crystallography III," ed by C. H. Macgillavry, G. D. Rieck, and K. Lonsdale, Kynoch Press (1962).

14) R. Mason, E. D. Mckensie, G. B. Robertson, and G. A. Rusholme, *J. Chem. Soc., Chem. Commun.*, **1969**, 56.

15) H. C. Freeman, G. H. Milburn, C. E. Nockolds, P. Hemmerich and K. H. Knauer, *J. Chem. Soc., Chem. Commun.*, **1969**, 56.

16) Trinh-Toan and L. F. Dahl, *J. Am. Chem. Soc.*, **93**, 2654 (1971).

17) J. W. Lauher and J. A. Ibers, *Inorg. Chem.*, **14**, 348 (1975).

18) B. Zaslow and R. E. Rundle, *J. Phys. Chem.*, **61**, 490 (1975).

19) M. J. Bennett, F. A. Cotton, and P. L. Weaver, *Acta Cryst.*, **23**, 581 (1967).

20) R. R. Richards and N. W. Gregory, *J. Phys. Chem.*, **69**, 239 (1965).

21) T. J. Kistenmacher and G. D. Stucky, *Inorg. Chem.*, **7**, 2150 (1968).

22) J. K. Beattje and C. J. Moore, *Inorg. Chem.*, **21**, 1292 (1982).

23) F. W. Kutzler, *SSRL Report*, **80/01**, (1981).

24) N. Kosugi, T. Yokoyama, K. Asakura, H. Kuroda, *Chem. Phys.*, **19**, 249 (1984).

25) H. Kuroda, N. Kosugi, K. Asakura, H. Ishii, M. Nomura, *Photon Factory Activity Report* **82/83**, VI-36, (1984).

26) The method of the deconvolution of the XPS peaks was described elwewhere.[27] The standard peaks used for Cl_{2p} and C_{1s} were the Cl_{2p} peak of $[N(C_2H_5)_4][FeCl_4]$ and C_{1s} peak of *trans*-polyacetylene, respectively.

27) I. Ikemoto, M. Yamada, T. Sugano, and H. Kuroda, *Bull. Chem. Soc. Jpn.*, **53**, 1871 (1980).

28) D. T. Clark, D. Kilcast, D. B. Adams and W. K. R. Musgrave, *J. Electron. Spec.*, **6**, 117 (1975).

29) I. Ikemoto, Y. Cao, M. Yamada, H. Kuroda, I. Harada, H. Shirakawa, and S. Ikeda, *Bull. Chem. Soc. Jpn.*, **55**, 721 (1982).